Int. J. Heat Mass Transfer. Vol. 29, No. 1, pp. 35–45, 1986
Printed in Great Britain

0017–9310/86 $3.00 + 0.00
Pergamon Press Ltd.

Frequency response of the mass transfer rate in a modulated flow at electrochemical probes

A. AMBARI, C. DESLOUIS and B. TRIBOLLET

LP 15 CNRS, Physique des Liquides et Electrochimie associé à l'Université Pierre et Marie Curie, 4 place Jussieu, 75230 Paris Cédex 05, France

(*Received* 25 *January and in final form* 8 *July* 1985)

Abstract—The transfer function between the mass flux on a microelectrode and the velocity gradient at the wall is numerically determined. A direct experimental measurement of this transfer function is performed on one hand for a modulated pipe flow and on the other hand for the modulated flow due to a rotating disk. In this last case, the accuracy of the data gives a good confirmation of the theory in the mid-frequency range and shows clearly a deviation, appearing in the high-frequency range, due to the fact that the electron transfer is not infinitely fast.

1. INTRODUCTION

ELECTROCHEMICAL probes which consist of microelectrodes acting as pure mass sink areas in the presence of a fast redox system, have been intended so far for hydrodynamical investigations, for instance to study the turbulent velocity gradient fluctuations near a wall [1–8], or for a direct comprehension of transient mass transfer phenomena occurring in pulsating blood circulation [9]. As to the former application, it is known that in the framework of a linear theory and assuming the time-dependent fluctuations as ergodic and the system as stationary from a statistical standpoint, the power spectrum density (PSD) of the mass flux $W_{\tilde{J}}$ and that of the velocity gradient $W_{\tilde{\alpha}}$ are linked through the following relationship [10, 11]:

$$W_{\tilde{J}} = \|H(jf)\|^2 W_{\tilde{\alpha}}. \tag{1}$$

For both applications, it is therefore important to determine accurately the transfer function $H(jf)$ which represents formally the linear response of the time-dependent mass transfer rate $\tilde{J}$ to a sine-wave modulation of low level of the wall velocity gradient $\tilde{\alpha}$. This is a similar problem to that of hot-wire anemometry, but owing to the high value of the Schmidt number Sc $(= \nu/D)$ in a fluid, the cut-off frequency of the mass transfer electrochemical probes is expected to be significantly lower than that of the thermal probes and hence a detailed knowledge of function $H(jf)$ is needed. $H(jf)$ had been previously calculated either numerically [12–16] or analytically [12, 16, 17].

In the earlier works, devoted primarily to blood circulation [9], the theoretical correlations were relative to pipe flows and indicated a reduction of the data by a dimensionless frequency $Sn \cdot Sc \cdot l^{+2/3}$ depending on the Stokes number $Sn\,(= R^2\omega/\nu$; R pipe radius and $\omega = 2\pi f)$ and on a dimensionless width l^+ of the active sensor $(= l/[2R \cdot Re\,Sc]$; l being the sensor dimension along the axis direction of the tube and Re the Reynolds number). Direct measurements by the polarographic technique in pipes with sinusoidally-modulated wall velocity gradients or pressure gradients, displayed data at variance with the analysis [9] or in a relatively satisfactory agreement [14] though some discrepancies in the latter work arose for the phase lag when a constant mass flux is chosen as boundary condition.

Fortuna and Hanratty provided an indirect verification of the variations of $H(jf)$ with frequency by considering, as perturbating flow, the turbulence itself and by analyzing the PSD of the mass transfer fluctuations, in a frequency range where the velocity spectrum was assumed as flat [12]. More recently, the calculations have been improved by taking into account the diffusion term in the longitudinal direction (mean flow direction), whose effect must be prevalent at the leading edge of the microelectrode [15].

Up to now, however, no conclusive and quantitative verification of those calculations has been given, mainly because the flow geometry investigated so far—i.e. the modulated pipe flow—is of a difficult setting.

In fact, the problem can be reduced by the use of a dimensionless frequency which appeals to local quantities such as the probe dimension l and the local wall velocity gradient $\bar{\alpha}$, so that any flow geometry should yield the same behavior.

Now, accurate mass transfer studies in modulated flow were recently carried out with a rotating disk electrode, a system which contains, in addition, a modulation of a velocity component perpendicular to the wall [18–20].

In this work, we develop, in the first part, the numerical calculation for the complete mass balance equation at a rectangular microelectrode and, hence, deduce the response of a circular microelectrode.

In the second part, the transient mass transfer data, collected for two modulated flow systems, i.e. the pipe flow and the rotating disk, are reported and compared with the theoretical values.

NOMENCLATURE

A amplitude
c concentration of the electroactive species [mol cm^{-3}]
c_∞ mean concentration of the electroactive species at infinity [mol cm^{-3}]
c_0 mean concentration of the electroactive species at the interface [mol cm^{-3}]
C double-layer capacity [Farad]
d diameter of circular microelectrode [cm]
D diffusion coefficient [cm^2 s^{-1}]
f frequency [Hz]
f^+ dimensionless frequency, $fl^{2/3}/D^{1/3}(\bar{\alpha})^{2/3}$
F dimensionless frequency, $\omega l^2/D$
H transfer function, $\tilde{J}/\tilde{\alpha}$ [see equation (1)]
I current [A]
j $\sqrt{-1}$
J diffusion or mass flux [cm^{-2} s^{-1}]
$\mathcal{J}_0, \mathcal{J}_1$ Bessel function of the first kind
k $\sqrt{\omega/\nu}$
K constant = 66.13 [see equation (17)]
l sensor width, [cm]
L sensor length [cm]
p dimensionless frequency, $\omega/\bar{\Omega}$
$\mathcal{P}$ dynamic pressure [N cm^{-2}]
r radial coordinate [cm]
R pipe radius [cm]
Re Reynolds number
R_T charge transfer resistance [Ω]
S Strouhal number, $f/\bar{\alpha}$
Sc Schmidt number, ν/D
Sn Stokes number, $R^2\omega/\nu$
t time [s]
u unsteady component of the velocity in a pipe along the axis direction [cm s^{-1}]
U mean value of the velocity in a pipe along the axis direction [cm s^{-1}]
v_r radial component of the fluid velocity [cm s^{-1}]
v_θ angular component of the fluid velocity [cm s^{-1}]
v_y component of the fluid velocity in the direction perpendicular to the wall [cm s^{-1}]
v_x component of the fluid velocity in the direction parallel to the wall [cm s^{-1}]
$W_{\tilde{\alpha}}$ power spectrum density of the velocity gradient
$W_{\tilde{j}}$ power spectrum density of the mass flux
x coordinate parallel to the wall (see Fig. 1)
y coordinate perpendicular to the wall (see Fig. 1)
z complex variable, $kRj^{3/2}$
Z electrochemical impedance [Ω]
Z_{EHD} electrohydrodynamical impedance (EHD)
Z_{HD} hydrodynamic transfer function
Z_D diffusion impedance [Ω].

Greek symbols
α local wall velocity gradient [s^{-1}]
β local constant [see equation (4)]
ε dimensionless velocity gradient [see equation (11)]
$\Gamma(4/3)$ = 0.89298, the gamma function of 4/3
γ constant [see equation (23)]
δ characteristic distance of the thickness of diffusion layer [cm]
ξ dimensionless axial distance, $y/\delta(x)$
$(-1/\theta'(0))$ dimensionless diffusion impedance
ρ density
ν kinematic viscosity [cm^2 s^{-1}]
ω modulation frequency [rad s^{-1}]
χ dimensionless parameter, $\alpha l^2/D$.

Superscripts
$\bar{}$ steady state
$\tilde{}$ unsteady component
$+$ dimensionless parameter.

2. STATEMENT OF THE PROBLEM

The concentration in the diffusion layer is governed by the unsteady equation of convective diffusion:

$$\frac{\partial c}{\partial t} + \vec{v} \cdot \vec{\text{grad}}\, c = D\nabla^2 c. \qquad (2)$$

The problem can always be reduced into a two-dimensional form by considering a rectangular microelectrode embedded in the wall of length L and width $l (L \gg l)$, with a local system of coordinates attached to the probe and such that its width is following the mean flow direction (Fig. 1).

In this configuration, the concentration derivatives

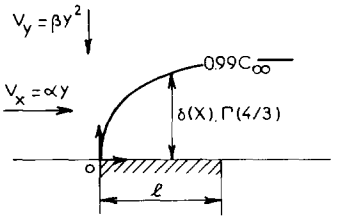

FIG. 1. Diffusion boundary layer over a rectangular microelectrode. For a pipe flow $\beta = 0$. For the flow due to a rotating disk $\beta < 0$ and in this last case the arrows indicate the direction of the velocity components. In some particular flows, as for example, the flow downstream a cylinder [6], β may be positive.

with respect to the transverse direction are a zero value and the convective term $\vec{v} \cdot \vec{\text{grad}}\, c$ is reduced to

$$v_x \frac{\partial c}{\partial x} + v_y \frac{\partial c}{\partial y}$$

where y is the distance from the wall and x is a coordinate along the local streamline.

If the dimensions of the microelectrode are small enough, we may assume that the gradient of the velocity component parallel to the wall is constant on the microelectrode area and that v_x is proportional to y in the diffusion layer above the microelectrode:

$$v_x = \alpha(x, t)y \tag{3}$$

and from the continuity equation:

$$v_y = \beta(x, t)y^2. \tag{4}$$

In the particular case of a bidimensional flow $\beta(x) = -1/2(\mathrm{d}\alpha/\mathrm{d}x)$, but this last relation is not verified for a three-dimensional flow as, for example, the flow due to a rotating disk.

For each frequency $\omega/2\pi$, every time-dependent parameter may be written in the following form:

$$X = \bar{X} + \text{real}\{\tilde{X} \exp \mathrm{j}\omega t\} \tag{5}$$

$\tilde{X}$ may be a complex quantity.

For a low-amplitude modulation of the velocity perturbation $|\tilde{\alpha}| \ll \bar{\alpha}$ and $|\tilde{\beta}| \ll \bar{\beta}$ the quadratic terms are negligible and the unsteady part of the convective diffusion equation is:

$$\mathrm{j}\omega\tilde{c} + \tilde{\alpha}y \frac{\partial \bar{c}}{\partial x} + \bar{\beta}y^2 \frac{\partial \tilde{c}}{\partial y} - D\left(\frac{\partial^2 \tilde{c}}{\partial x^2} + \frac{\partial^2 \tilde{c}}{\partial y^2}\right) = -\tilde{\alpha}y \frac{\partial \bar{c}}{\partial x} - \bar{\beta}y^2 \frac{\partial \bar{c}}{\partial y}. \tag{6}$$

For a microelectrode, Mollet *et al.* [21] showed that the condition, $|\beta l/\alpha| \ll 1$, is equivalent to the condition

$$v_y \frac{\partial c}{\partial y} \ll v_x \frac{\partial c}{\partial x},$$

so for a microelectrode small enough equation (6) becomes:

$$\mathrm{j}\omega\tilde{c} + \tilde{\alpha}y \frac{\partial \bar{c}}{\partial x} - D\left(\frac{\partial^2 \tilde{c}}{\partial x^2} + \frac{\partial^2 \tilde{c}}{\partial y^2}\right) = -\tilde{\alpha}y \frac{\partial \bar{c}}{\partial x}. \tag{7}$$

Ling [22] normalized all the distances by using the width l: $x^+ = x/l$, $y^+ = y/l$.

$$\mathrm{j}\frac{\omega l^2}{D}\tilde{c} + \frac{\tilde{\alpha}l^2}{D} y^+ \frac{\partial \tilde{c}}{\partial x^+} - \left(\frac{\partial^2 \tilde{c}}{\partial x^{+2}} + \frac{\partial^2 \tilde{c}}{\partial y^{+2}}\right) = -\frac{\tilde{\alpha}l^2}{D} y^+ \frac{\partial \bar{c}}{\partial x^+}. \tag{8}$$

In the stationary case, only one dimensionless parameter appears: $\chi = \bar{\alpha}l^2/D$ and Ling [22] had shown that for $\bar{\alpha}l^2/D > 5000$ the diffusion in the x direction can be neglected.

In the non-stationary case a second dimensionless parameter appears: $F = \omega l^2/D$.

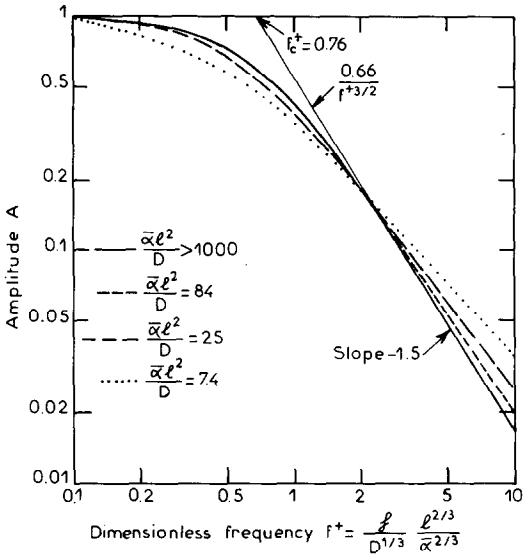

FIG. 2. Numerical calculation of the amplitude A of the transfer function H vs the dimensionless frequency f^+. The asymptotic behavior $A = 0.66/f^{+3/2}$ is indiscernible at high frequencies from the numerical calculation for $\bar{\alpha}l^2/D > 1000$.

2.1. *Numerical integration*

The unsteady equation of convective diffusion (6) is numerically integrated by using Newman's method [23, 24]. The integration is done, after modification of the equation (6) by the dimensionless parameter: $\xi = y/\delta(x)$, where $\delta(x)$ is a distance characteristic of the thickness of the steady-state diffusion layer [21, 25]:

$$\delta(x) = \left(\frac{3D}{\bar{\beta}}\right)^{1/3} \left(\exp \frac{3\bar{\beta}x}{\bar{\alpha}} - 1\right)^{1/3}. \tag{9}$$

With the dimensionless parameter ξ, the equation becomes more complicated but the integration may be done with a constant mesh size.

The results are given in Fig. 2; the amplitude of the transfer function $H = \tilde{J}/\tilde{\alpha}$ is normalized by its value when the frequency tends towards zero.

For $\bar{\alpha}l^2/D > 1000$ all the curves are reduced by a dimensionless frequency f^+ where:

$$f^+ = \frac{f}{D^{1/3}} \frac{l^{2/3}}{\bar{\alpha}^{2/3}} \tag{10}$$

and a good agreement is found with the previous integration [12, 16]. We notice that f^+ may be expressed as a combination of the two dimensionless parameters defined from (8) ($f^+ = F\chi^{-2/3}/2\pi$) or f^+ may be also expressed by using the Strouhal number $S = f/\bar{\alpha}$ ($f^+ = S\chi^{1/3}$).

When $\alpha l^2/D$ decreases, different curves are obtained and the slope in the high-frequency range increases from -1.5.

The instantaneous wall velocity gradient $\tilde{\alpha}$ is not accessible by usual techniques and will be therefore experimentally referred to a phase origin corresponding to the location of the flow perturbation.

In a linear theory, the dimensionless perturbation $\varepsilon(\omega) = \tilde{\alpha}/\bar{\alpha}$ is such that $|\varepsilon(\omega)| \ll 1$ as assumed above. $\varepsilon(\omega)$ is a complex number and its phase shift is a function of the flow. The exact determination of $\varepsilon(\omega)$ will be given for each particular flow in the following.

2.2. *Asymptotic behavior of transfer function* H

In this section, high-frequency and low-frequency regimes will be defined with respect to f^+. From Figure 2, the low-frequency regime is valid for $f^+ < 0.1$ and the high-frequency regime corresponds to $f^+ > 2$. These values are corroborated by the phase shift variations. For the low-frequency range considered, the instantaneous fluxes and velocity gradient are in phase and for the high-frequency range a limiting phase shift of $-3\pi/4$ is observed.

In a previous work [26] asymptotic behaviors of the mass transfer responses for a rotating disk electrode have been calculated in the low- and high-frequency domains, respectively. These results may be extended to the microelectrodes when the diffusion in the x direction is neglected and when the concentration of electroactive species at the interface is zero.

In the low-frequency range, i.e. in quasi-steady state, the instantaneous fluxes and velocity gradient are in phase. The overall flux on the microelectrode is from [26]:

$$\langle \tilde{J}_{LF} \rangle = \frac{DL\tilde{\alpha}(0)}{3\bar{\alpha}} \int_0^l \left.\frac{d\tilde{c}}{dy}\right|_0 dx = \frac{DL\tilde{\alpha}(0)}{3\bar{\alpha}} \int_0^l \frac{dx}{\delta(x)} \quad (11)$$

$\delta(x)$ is given by (9). The quantity $3\beta l/\bar{\alpha}$ is negligible for a disk, and is equal to zero for a pipe flow, and equation (9) becomes:

$$\delta(x) = \left(\frac{9Dx}{\bar{\alpha}}\right)^{1/3} \quad (12)$$

and then:

$$H_{LF} = \frac{\langle \tilde{J}_{LF} \rangle}{\tilde{\alpha}(0)} = \frac{LD}{2\bar{\alpha}} \frac{c_\infty - c_0}{\Gamma(4/3)} l \left(\frac{\bar{\alpha}}{9Dl}\right)^{1/3}. \quad (13)$$

In the high-frequency range, from [26], the local flux may be expressed by:

$$D \left.\frac{\partial \tilde{c}}{\partial y}\right|_0 = D \frac{\tilde{\alpha}}{\bar{\alpha}} \left.\frac{\partial \bar{c}}{\partial y}\right|_0 6 \Big/ \left[j \frac{\omega \delta^2(x)}{D}\right]^{3/2} \quad (14)$$

and the transfer function for the microelectrode is:

$$H_{HF} = \frac{LD}{\bar{\alpha}} \int_0^l \left.\frac{\partial \tilde{c}}{\partial y}\right|_0 dx = -6 \frac{LD}{\bar{\alpha}} \frac{c_\infty - c_0}{\Gamma(4/3)} j^{1/2} \times \left(\frac{D}{\omega}\right)^{3/2} \int_0^l \frac{dx}{\delta^4(x)}. \quad (15)$$

The integral $\int_0^l dx/\delta^4(x)$ diverges, this problem was not mentioned in the previous works. This divergence occurs because $\partial^2 c/\partial x^2$ cannot be neglected as regards to $\partial^2 c/\partial y^2$ close to the leading edge of microelectrode, and the actual concentration profile would be of the power law type but with an exponent smaller than 1/3.

From the numerical integration (Fig. 2), it emerges that:

$$\frac{H_{HF}}{H_{LF}} = \frac{0.66}{f^{+3/2}}. \quad (16)$$

Returning to the HF solution, it can be inferred, that, on the basis of dimensional arguments, H_{HF} takes the following expression:

$$H_{HF} = KLD \frac{c_\infty - c_0}{\Gamma(4/3)} j^{1/2} \left(\frac{D}{\omega}\right)^{3/2} l \left(\frac{\bar{\alpha}}{9Dl}\right)^{4/3} \quad (17)$$

with $K = 66.13$.

The cut off frequency defined by $H_{HF}/H_{LF} = 1$ is $f_c^+ = 0.758$.

2.3. *Circular microelectrode*

In order to determine the frequency response of a circular microelectrode (diameter d) from the asymptotic behavior established for a rectangular microelectrode, we used the method described in [21] for the stationary case.

For a rectangular microelectrode as described at the beginning of this paper, all concentration derivatives with respect to the z direction are a zero value; for a circular microelectrode we assume that the diffusion in the z direction may be neglected. This assumption was verified in the stationary case [21]: on the basis of experimental considerations we will show further that it can be extended to the transient case.

The length L is substituted by t and the value dJ is integrated on the overall surface of the circular microelectrode:

$$\langle \tilde{J}_{LF} \rangle = \frac{D\varepsilon(0)}{2} \frac{c_\infty - c_0}{\Gamma(4/3)} \left(\frac{\bar{\alpha}}{9D}\right)^{1/3} \times 2 \int_0^{d/2} \left(2\sqrt{\frac{d^2}{4} - t^2}\right)^{2/3} dt \quad (18)$$

$$\langle \tilde{J}_{LF} \rangle = 0.2019\varepsilon(0) \frac{c_\infty - c_0}{\Gamma(4/3)} (\bar{\alpha})^{1/3} D^{2/3} d^{5/3}. \quad (19)$$

By the same procedure one finds:

$$\langle \tilde{J}_{HF} \rangle = 3.92105 j^{1/2} \varepsilon(\omega) \frac{c_\infty - c_0}{\Gamma(4/3)} \frac{D^{7/6} (\bar{\alpha})^{4/3} d^{2/3}}{\omega^{3/2}} \quad (20)$$

and therefore

$$|\langle \tilde{J}_{HF} \rangle| = 2.7726\varepsilon(\omega) \frac{c_\infty - c_0}{\Gamma(4/3)} \frac{D^{7/6} (\bar{\alpha})^{4/3} d^{2/3}}{\omega^{3/2}}. \quad (21)$$

The following expression is then obtained for the circular microelectrode:

$$\frac{|\langle \tilde{J}_{HF} \rangle|}{|\langle \tilde{J}_{LF} \rangle|} = 0.8719 \frac{\varepsilon(\omega)}{\varepsilon(0)} \frac{D^{1/2} \bar{\alpha}}{f^{3/2} d}. \quad (22)$$

By assuming the same relationship as that given in equation (16), one has to consider the circular microelectrode as a rectangular one whose width would be equal to $0.756d$. In the stationary case, the behavior of a circular microelectrode was similar to that of a rectangular one whose width was set equal to $0.81d$ [21].

3. EXPERIMENTAL RESULTS AND DISCUSSION

3.1. *Modulated pipe flow*

We first studied the response of an electrochemical circular probe embedded in a circular pipe to a sine-wave modulation of the flow velocity.

The fluid was circulated through a circular pipe of diameter $2R = 2.5$ cm and length 3 m between two tanks by imposing a constant and controlled pressure P in the upstream tank (see Fig. 3), whereas the downstream tank was allowed to reach atmospheric pressure P_{at}. Since laminar conditions were required, the flow rate was decreased by putting in the upstream region a circular disk (1 in Fig. 3) in the cross section of the pipe, drilled with small holes ($\varnothing = 0.5$ mm) regularly spaced and the viscosity was increased as well by adding glucose to the fluid. The distance between the upstream disk and the downstream electrochemical test section was large enough so that a completely Poiseuille profile was established. The flow rate was modulated by means of a piston submitted to a linear sinusoidally-alternating motion provided by a pushing rod (see Fig. 3).

The flow rate was measured by using a flowmeter (CROUZET). In transient conditions, the fluctuating flow rate was found to be practically in phase with the fluctuating velocity along the symmetry axis of the pipe. The electric signal delivered by this device triggered the generator of a transfer function analyzer (1172 SOLARTRON): the transfer function between the modulated response of the diffusion flux and the instantaneous velocity on the pipe axis was then analyzed as function of frequency. However, this transfer function equal to $\tilde{J}/\tilde{u}$ (axis) deviates from the calculated transfer function $\tilde{J}/\tilde{\alpha}$ given by the numerical analysis. Indeed, since

$$\tilde{J}/\tilde{\alpha} = \{\tilde{J}/\tilde{u}(\text{axis})\}\,\{\tilde{u}(\text{axis})/\tilde{\alpha}\},$$

one has to calculate the transfer function $\tilde{u}(\text{axis})/\tilde{\alpha}$. This was done according to the work by Uchida [27], who calculated the modulated velocity in a circular pipe due to a fluctuating pressure gradient of the form:

$$\frac{\partial \tilde{p}}{\partial x} = \gamma \frac{\partial \bar{p}}{\partial x} \exp j\omega t \quad \text{with} \quad \gamma \ll 1. \tag{23}$$

He then found:

$$\tilde{u}(r) = \frac{j}{\rho\omega}\left\{1 - \frac{\mathscr{J}_0(krj^{3/2})}{\mathscr{J}_0(kRj^{3/2})}\right\}\frac{\partial \bar{p}}{\partial x}\gamma \exp j\omega t \tag{24}$$

where r is the radial distance starting from the pipe axis; $k^2 = \omega/\nu$; ρ is the density; $\partial\bar{p}/\partial x$ the mean pressure gradient. $\mathscr{J}_0$ is the Bessel function of the first kind.

It readily emerges that:

$$\frac{\tilde{u}(\text{axis})}{\tilde{\alpha}} = \frac{R[1-\mathscr{J}_0(z)]}{z\mathscr{J}_1(z)} \tag{25}$$

with $z = kRj^{3/2}$.

The argument of the complex variable z has a constant value of $3\pi/4$ and therefore, any Bessel function of the first kind can be expressed in terms of the Kelvin functions ber and bei:

$$\mathscr{J}_n(z) = \text{ber}(z) + j \cdot \text{bei}(z)$$

which have been tabulated in [28].

The transfer function $\tilde{u}(\text{axis})/\tilde{\alpha}$ is plotted in Bode coordinates in Fig. 4. A limiting phase shift value of 45° is reached.

The electrochemical reaction due to the tri-iodide/iodine system ($I_3^- + 2e^- \leftrightarrows 3I^-$) evolved on a circular platinum microelectrode ($d = 0.5$ mm) embedded flush with the insulated wall of the pipe. The limiting diffusion current corresponding to the reduction step of the reaction was measured by means of a current-to-voltage converter (which provides a less

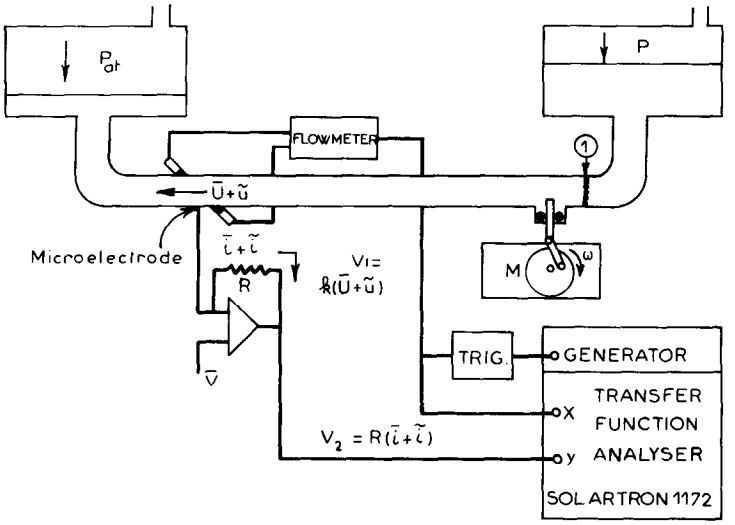

FIG. 3. Experimental device for the pulsating flow in a pipe flow.

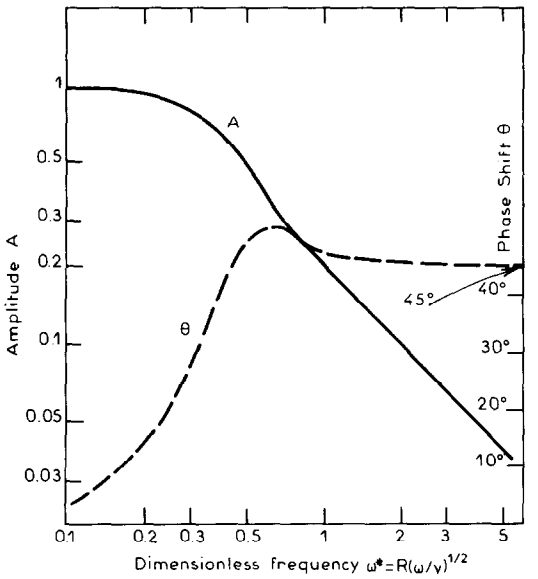

FIG. 4. Theoretical hydrodynamic transfer function between the velocity on the axis of the pipe and the wall velocity gradient. The amplitudes are normalized by the value of the amplitude when the frequency tends towards zero.

noisy signal than that observed with a usual potentiostat (Fig. 3).

The physicochemical parameters of the solution were determined as:

$$\nu = 2.1 \times 10^{-2}\ \text{cm}^2\ \text{s}^{-1}$$

$$D = 4.48 \times 10^{-6}\ \text{cm}^2\ \text{s}^{-1}.$$

Three experiments performed at $\bar{U} = 5.67$, 8.1 and 8.9 cm s^{-1} enabled us to compare the experimental response with the theoretical values given in the first section.

In Fig. 5 we represented the phase shift vs the dimensionless frequency f^+.

As predicted from the theoretical section, we assume that a circular microelectrode is equivalent to a rectangular microelectrode of width $l = 0.756d$.

A certain scattering of the data is observed due to the difficulty in performing such measurements at frequencies below 1 Hz (this corresponds to a low rotation frequency of the DC motor which drives the piston). However, the theoretical curve (full line) passes through experimental data and the agreement is quite satisfactory. When one tries to analyze the amplitude data (Fig. 6), a problem arises due to the fact that low-frequency modulations could not be achieved so that the low-frequency plateau was not obtained and the normalization procedure failed. However, the asymptotic behavior of the amplitude A at high frequencies—i.e. a power law correlation of the type $A \propto f^{+-1.5}$—is consistent with the theoretical predictions (the values of $\bar{\alpha}l^2/D$ investigated were higher than 10^4) and tends to indicate a low influence of the longitudinal term in the Laplacian [equation (7)].

3.2. *Modulated flow at a rotating disk*

The use of a modulation flow technique has been recently developed in electrochemistry to analyze the coupling between mass transfer and the interfacial kinetics associated to the electron transfer [18–20]. It consists in studying the frequency response of the diffusion flux to a low-level sinusoidal speed modulation of the disk superimposed to a time-average value.

The transfer function experimentally determined is the ratio $\tilde{J}/\tilde{\Omega}$ where $\tilde{\Omega}$ is the amplitude of the velocity modulation as expressed by equation (5).

As previously done for the pipe flow, this experimentally accessible quantity differs from the

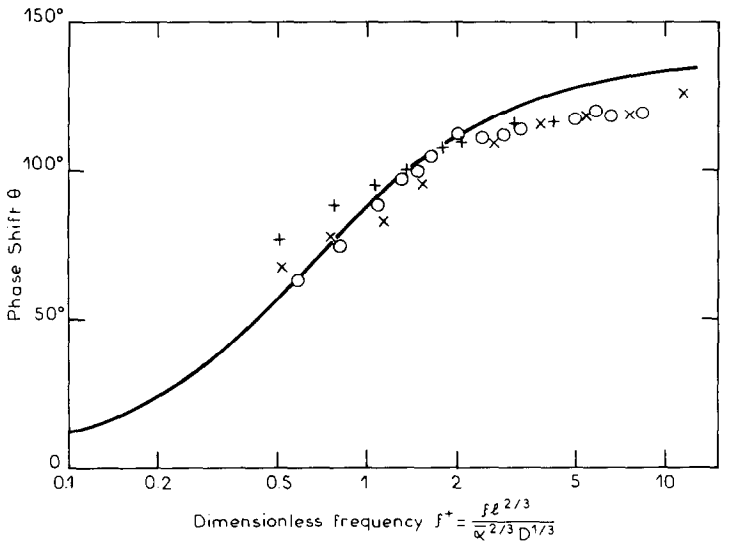

FIG. 5. Experimental phase shift of the mass transfer attenuation $H(2\pi f)$ vs the dimensionless frequency for the pulsating pipe flow.

predicted quantity $H = \tilde{J}/\tilde{\alpha}$ by an additional transfer function $Z_{HD} = \tilde{\alpha}/\tilde{\Omega}$ with

$$\frac{\tilde{J}}{\tilde{\Omega}} = \frac{\tilde{J}}{\tilde{\alpha}} \cdot Z_{HD}.$$

Z_{HD} is a complex quantity proportional to $\varepsilon(\omega)/\varepsilon(0)$. The fluctuating velocity components $\tilde{v}_y$, $\tilde{v}_r$ and $\tilde{v}_\theta$ were numerically calculated for a rotating disk in ref. [20]. Analytical expressions had been previously established either in the low-frequency [29] or in the high-frequency ranges [30].

In the local system of coordinates where x defines the tangential direction to the streamline, then:

$$\bar{v}_x = (\overline{v_r}^2 + \overline{v_\theta}^2)^{1/2}$$

and

$$\tilde{v}_x = \frac{\tilde{v}_r \bar{v}_r + \tilde{v}_\theta \bar{v}_\theta}{\bar{v}_x} \tag{26}$$

where v_r and v_θ are the usual radial and tangential velocities in a cylindrical system of coordinates.

The variations of $\varepsilon(p)/\varepsilon(0)$ with the dimensionless frequency $p(=\omega/\Omega)$, were calculated by means of equation (26) from the theoretical values of $\tilde{v}_r$ and $\tilde{v}_\theta$ predicted in ref. [20], and are reported in Fig. 7: from [29, 30], we deduced approximate expressions of $\varepsilon(p)/\varepsilon(0)$ for the low-frequency range

$$\frac{\varepsilon(p)}{\varepsilon(0)_{p\to 0}} \simeq 1 + 0.12808 \mathrm{j} p \tag{27}$$

and for the high-frequency range:

$$\frac{\varepsilon(p)}{\varepsilon(0)} \simeq \left(0.4539\sqrt{p} + \frac{0.3760}{\sqrt{p}}\right) + \mathrm{j}\left(0.4539\sqrt{p} - \frac{0.376}{\sqrt{p}} - \frac{0.3247}{p}\right). \tag{28}$$

The electronic device used for the control of the limiting diffusion currents is the same as that schematized in Fig. 3 and the mechanical set-up has been described in [31].

The modulation is generated by a DC motor, the angular velocity of which is servo-controlled to within 0.1%. This velocity can be changed very quickly due to a very low inertia; frequency modulations as high as 130 Hz could be reached with a modulation ratio $\tilde{\Omega}/\bar{\Omega}$ of 10% at any time-average value $\bar{\Omega}$ between 20 and 5000 rpm.

Since no experimental checking of the validity of the theoretical prediction concerning the transfer function Z_{HD} for a rotating disk has been given so far, it was necessary to devise appropriate experimental conditions so as to separate the effects of $Z_{EHD} = \tilde{J}/\tilde{\Omega}$ and $\tilde{J}/\tilde{\alpha}$.

For a rotating disk, the velocity gradient is $\bar{\alpha} = 0.8\ \Omega^{3/2}\ \nu^{-1/2}\ r$ and then it is convenient to put the general dimensionless frequency f^+ [equation (10)]

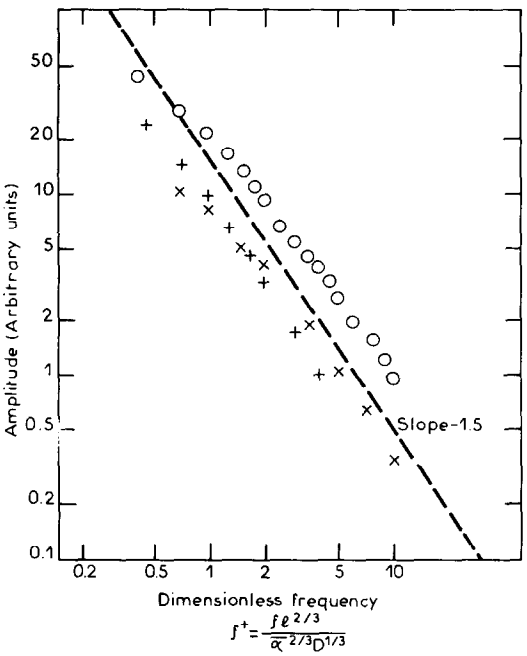

FIG. 6.

in the following form:

$$f^+ = 0.963\ p\ Sc^{1/3}\left(\frac{d}{r}\right)^{2/3}. \tag{29}$$

In contrast, it must be emphasized that Z_{HD} is only dependent on p.

We therefore embedded, in an insulated disk plane, microelectrodes of different diameters ($50\ \mu < d < 150\ \mu$) and distances from the rotation axis ($1.5\ \text{mm} < r < 27\ \text{mm}$).

The Schmidt number was also increased by mixing glycerol with the solution which increased the viscosity.

Hydrodynamic transfer function Z_{HD}. For the most remote electrode from the rotation axis, the term $(d/r)^{2/3}$ is very small and over a meaningful range of p, f^+ remains much smaller than one. Therefore, $\tilde{J}/\tilde{\alpha}$ introduces no attenuation and the observed response comes mainly from Z_{HD}.

In Fig. 7, the experimental amplitude and phase shift of $\tilde{J}/\tilde{\Omega}$ for the microelectrode ($d = 80\ \mu\text{m}$; $r = 27\ \text{mm}$) in a solution of KCl (M) at 20°C ($Sc \simeq 1200$) have been plotted and compared to the theoretical variation of Z_{HD}. The agreement is excellent, especially for the amplitudes up to $p \simeq 10$ whereas the phase shift displays a divergence at lower p values. The deviation appearing beyond, marks the beginning of the attenuation of $\tilde{J}/\tilde{\alpha}$. If the Schmidt number is increased, with the same geometry, the mass transport attenuation occurs sooner as displayed in Fig. 8 where a 50–50 water–glycerol mixture was used ($Sc \simeq 22\,000$).

Mass transfer attenuation $\mathrm{H} = \tilde{J}/\tilde{\alpha}$. Microelectrodes located near the rotation axis were also used, in order to increase the term $(d/r)^{2/3}$. However in all cases, the effect

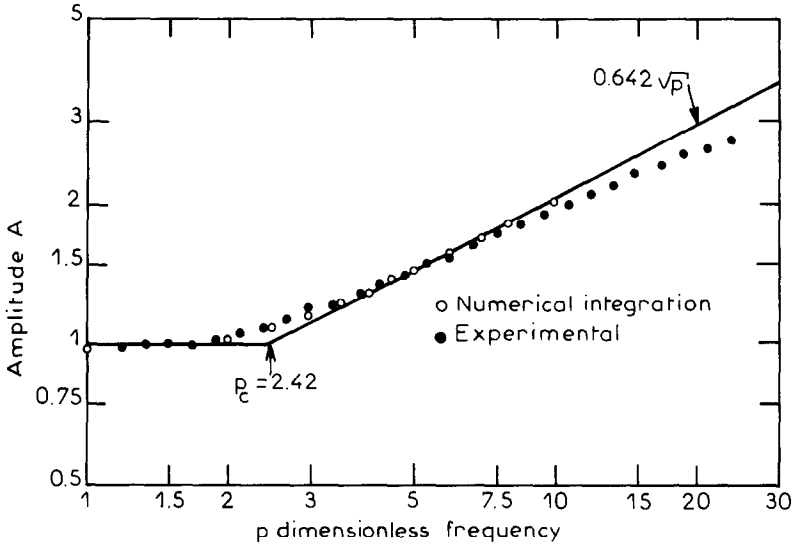

FIG. 7(a). Amplitude of the theoretical hydrodynamic transfer function $Z_{HD}(0)$ [equation (28)]. ○ Experimental data of Z_{EHD} with $d = 8 \times 10^{-3}$ cm, $r = 2.7$ cm, $Sc = 1200$. The amplitudes are normalized by $A(0)$.

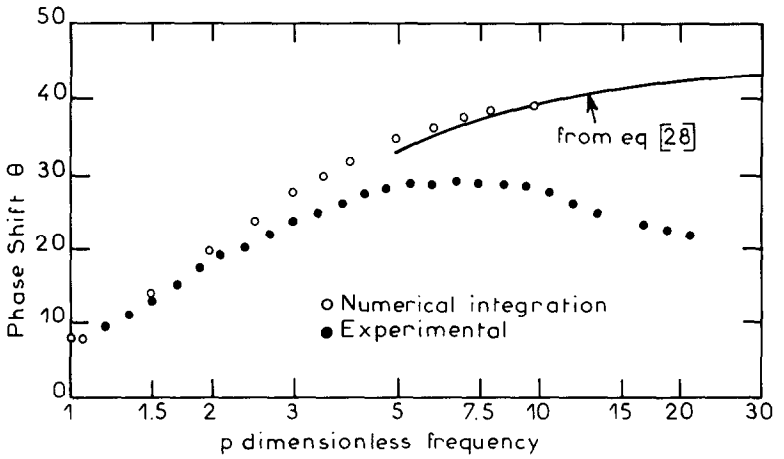

FIG. 7(b). Phase shift of the same quantities as in Fig. (a).

of Z_{HD} could not be disregarded and the data were therefore corrected from its effect so as to analyze the H variations alone. These data are plotted in Fig. 9 vs f^+. In a significant range of frequency there is a very satisfactory fit of the theoretical curve to the experimental data and this last set of measurements definitely yields a good confirmation of the theoretical predictions.

However, in the high-frequency range, the experimental data fall well below the theoretical curve, a fact which had been previously noticed with a rotating disk electrode [20]. Indeed, up to now, we assumed the instantaneous diffusion current I as proportional to the diffusion flux J, i.e. the electron transfer is infinitely fast with respect to the mass transfer process in non-steady-state conditions. In other words, this means that the measured overall transfer function $\tilde{I}/\tilde{\Omega}$ contains

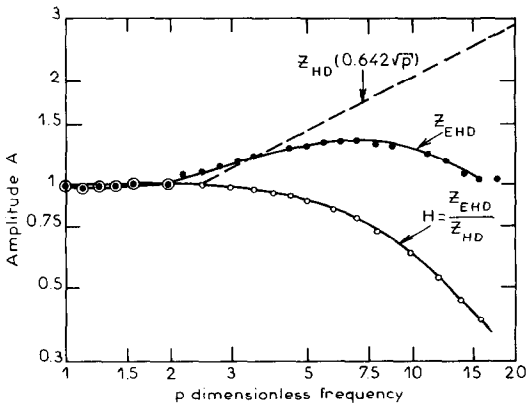

FIG. 8. Determination of the mass transfer attenuation H from the experimental measurement of Z_{EHD} ($= \tilde{J}/\tilde{\Omega}$) and by using the Z_{HD} values.

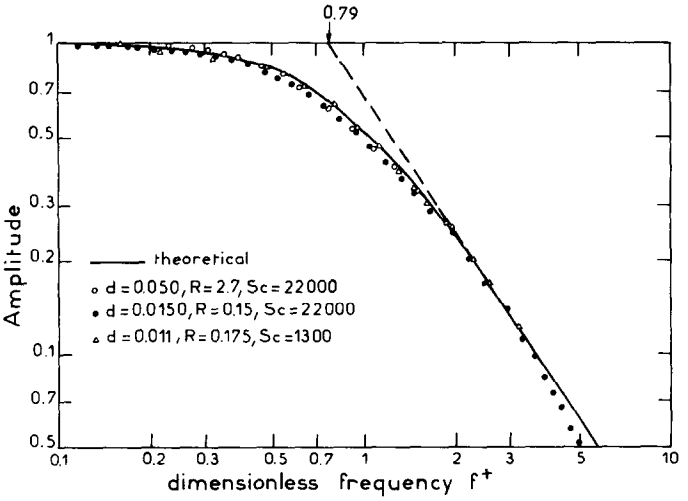

FIG. 9. Variations of the amplitude of the mass transfer attenuation H obtained from the Z_{EHD} measurements in different experimental conditions vs the dimensional frequency f^+.

another intermediate transfer function $\tilde{I}/\tilde{J}$ which is a pure real number only at zero frequency or at low frequencies: such a behavior had not been considered in the previous work dealing with electrochemical experiments.

The analysis derived for a rotating disk electrode in [20], led to the following equation and can be extended to the microelectrode:

$$\frac{\tilde{I}}{\tilde{J}} = \frac{\bar{I}}{\bar{J}} \frac{1}{1+j\omega C(R_T+Z_D)} \frac{Z_D}{Z} \qquad (30)$$

C is the double-layer capacitance with a usual value of the order of 50 μF cm^{-2}. R_T is the charge-transfer resistance which decreases as the rotation is increased. Z_D is the diffusion impedance and can be written as

$$\frac{R_D}{\Gamma(4/3)}\left[-\frac{1}{\theta'(0)}(\omega)\right]$$

where R_D, the diffusion resistance, is such that $R_D \gg R_T$. The expression of $[-1/\theta'(0)\cdot(\omega)]$ is given in [32, 33] and in particular:

$$\left[-\frac{1}{\theta'(0)}(\omega)\right] \to \Gamma(4/3) \quad \text{when} \quad \omega \to 0$$

$$\left[-\frac{1}{\theta'(0)}(\omega)\right] \to 0 \quad \text{when} \quad \omega \to \infty.$$

4. CONCLUSIONS

In the present work, it has been shown that electrochemical probes based on a mass transfer measurement are useful tools intended for the analysis of wall velocity gradient instabilities provided that their transfer function in a linear sine-wave modulated flow is known. This function was calculated in the general case of a two-dimensional velocity field near the wall and by considering the complete mass balance equation.

It was demonstrated that the numerical coefficient allowing the formal equivalence of a circular probe with a rectangular one is somewhat smaller than that calculated in steady flow conditions.

Two modulated flows were investigated: the pipe flow and the flow around a rotating disk. The frequency analysis of the experimental transfer function fulfilled very satisfactorily the theoretical predictions especially for the rotating disk flow, the experimental conditions of which could be very well controlled.

However, and at variance with the steady-state problem, the electron transfer process of the electrochemical reaction could not be considered as infinitely fast with respect to the mass transfer process at the highest frequencies investigated. This fact was not mentioned so far in the earlier contributions and some suggestions have been given in this paper in order to predict the observed deviations. A more quantitative treatment involving the electrochemical parameters of the reaction used is in progress.

REFERENCES

1. L. P. Reiss and T. J. Hanratty, An experimental study of the unsteady nature of the viscous sublayer, *A.I.Ch.E. J.* **9**, 154 (1963).
2. L. P. Reiss, Investigation of turbulence near a pipe wall using a diffusion controlled electrolytic reaction on a circular electrode. Ph.D. thesis, University of Illinois, Urbana (1962).
3. B. Py et J. Gosse, Sur la réalisation d'une sonde polarographique sensible à la vitesse et à la direction de l'écoulement, *C.r. Acad. Sci. Paris* **269**, 401–405 (1969).
4. M. Lebouche et G. Cognet, La polarographie, moyen d'étude du mouvement des liquides, *Chim. Ind.* **97**, 2002 (1967).
5. M. Lebouche, Relation entre les fluctuations pariétales du transfert massique et du gradient de vitesse dans le cas d'un nombre de Schmidt grand, *C.r. Acad. Sci. Paris* **271**, 438–441 (1970).
6. M. Lebouche et M. Martin, Convection forcée autour du cylindre, sensibilité aux pulsations de l'écoulement externe, *Int. J. Heat Mass Transfer* **18**, 1161–1175 (1975).

7. M. Martin, M. Lebouche et J. Gosse, Etude de la phase du transfert pariétal de chaleur ou de masse en écoulement incompressible, IUTAM Symposium, Laval, Québec, Canada (1972).
8. A. Ambari, C. Deslouis and B. Tribollet, Mass transfer and polymer—flow interactions close to a wall in elongational and turbulent flows, Drag Reduction 84, BHRA, Bristol, U.K. (1984).
9. R. D. Patel, J. J. McFeely and K. R. Jolls, Wall mass transfer in laminar pulsatile flow in a tube, *A.I.Ch.E. J.* **21,** 259 (1975).
10. C. Deslouis, B. Tribollet and L. Viet, The correlation between momentum and mass transfer for a turbulent or periodic flow in a circular pipe by electrochemical methods, *4th Int. Conference on Physicochemical Hydrodynamics, Ann. N. Y. Acad. Sci.* **404,** 471 (1983).
11. V. E. Nakoryakov, O. N. Kashinsky and B. K. Kozmenko, Electrochemical method for measuring turbulent characteristics of gas–liquid flows, Measuring Techniques in Gas–Liquid Two–Phase Flows, IUTAM Symposium, Nancy, France (1983).
12. G. Fortuna and T. J. Hanratty, Frequency response of the boundary layer on wall transfer probes, *Int. J. Heat Mass Transfer* **14,** 1499 (1971).
13. B. Py, Etude tridimensionnelle de la sous-couche visqueuse dans une veine rectangulaire par des mesures de transfert de matière en paroi, *Int. J. Heat Mass Transfer* **16,** 129 (1973).
14. T. Mizushina, T. Maruyama, S. Ide and Y. Mizukami, Dynamic behaviour of transfer coefficient in pulsating laminar tube flow, *J. chem. Engng. Jap.* **6,** 152 (1973).
15. J. Y. Dumaine, Etude numérique de la réponse en fréquence des sondes électrochimiques, *Lett. Heat Mass Transfer* **8,** 293 (1981).
16. T. J. Hanratty and J. A. Campbell, Measurement of wall shear stress. In *Fluid Mechanics Measurements*, edited by R. J. Goldstein. Hemisphere, Washington (1983).
17. J. E. Mitchell and T. J. Hanratty, A study of turbulence at wall using an electrochemical wall shear stress meter, *J. Fluid Mech.* **26,** 199 (1966).
18. W. J. Albery, A. R. Hillman and S. Bruckenstein, Hydrodynamic modulation at a rotating disc electrode, *J. electroanal. Chem.* **100,** 687 (1979).
19. C. Deslouis, C. Gabrielli, Ph. Sainte Rose Fanchine and B. Tribollet, Electrohydrodynamical impedance on a rotating disk electrode—I. Redox system, *J. electrochem. Soc.* **129,** 107 (1982).
20. B. Tribollet and J. Newman, The modulated flow at a rotating disk electrode, *J. electrochem. Soc.* **130,** 2016 (1983).
21. L. Mollet, P. Dumargue, M. Daguenet et D. Bodiot, Calcul du flux limite de diffusion sur une microélectrode de section circulaire—équivalence avec une électrode de section rectangulaire. Vérification expérimentale dans le cas du disque tournant en régime laminaire, *Electrochim. Acta* **19,** 841 (1974).
22. S. C. Ling, Heat transfer from a small isothermal span wise strip on an insulated boundary, *Trans. Am. Soc. mech. Engrs*, Series C, *J. Heat Transfer* **85,** 230 (1963).
23. J. Newman, *Electrochemical Systems.* Prentice Hall, Englewood Cliffs, N.J. (1973).
24. J. Newman, Numerical solution of coupled, ordinary differential equations, *Ind. Engng Chem.* **7,** 514 (1968).
25. G. Cognet, Utilisation de la polarographie pour l'étude de l'écoulement de Couette, *J. Méc.* **10,** 69–90 (1971).
26. C. Deslouis and B. Tribollet, Mass transfer for a modulated flow at a rotating disk electrode: asymptotic solutions, *J. electroanal. Chem.* **185,** 171–176 (1985).
27. S. Uchida, The pulsating viscous flow superposed on the steady laminar motion of incompressible fluid in a circular pipe, *Z. angew. Math. Mech.* **7,** 403 (1956).
28. M. Abramowitz and I. Stegun, *Handbook of Mathematical Functions.* Dover, New York (1972).
29. E. M. Sparrow and J. L. Gregg, Flow about unsteadily rotating disk, *J. Aerospace Sci.* **27,** 252 (1960).
30. V. P. Sharma, Flow and heat transfer due to small torsional oscillations of a disk about a constant mean, *Acta mech.* **32,** 19 (1979).
31. C. Deslouis, C. Gabrielli and B. Tribollet, A new device for EHD impedance measurement in the high frequency range. Applications to corrosion, 166th Meeting of ECS, New Orleans, October 1984 (Abstract no. 261).
32. B. Tribollet and J. Newman, Analytic expression of the Warburg Impedance for a rotating disk electrode, *J. electrochem. Soc.* **130,** 822 (1983).
33. C. Deslouis, C. Gabrielli and B. Tribollet. An analytical solution of the nonsteady convective diffusion equation for rotating electrodes, *J. electrochem. Soc.* **130,** 2044 (1983).

REPONSE EN FREQUENCE DU TRANSPORT DE MATIERE SUR DES SONDES ELECTROCHIMIQUES EN ECOULEMENT MODULE

Résumé— La fonction de transfert entre le flux de matière sur une microélectrode et le gradient de vitesse à la paroi est déterminée numériquement. Une mesure expérimentale directe de cette fonction de transfert est effectuée d'une part pour l'écoulement modulé dans un tuyau et d'autre part pour l'écoulement modulé au voisinage d'un disque tournant. Dans ce dernier cas, la précision des résultats donne une bonne confirmation de la théorie dans le domaine des fréquences intermédiaires. L'écart observé dans le domaine haute fréquence a été attribué au fait que le transfert d'électrons n'est pas infiniment rapide.

FREQUENZGANG DES STOFFTRANSPORT AUF ELECTROCHEMISCHEN SONDEN FUR ZEITLICH MODULIERTE STROMUNGEN

Zusammenfassung—Die Ubertragungsfunktion zwischen dem Stoffluß auf einer Mikroelectrode und dem Geschwindigkeits-Gefälle bei der Wand wird numerisch erechnet. Die experimentelle Messung dieser Funktion erfolgte durch zwei zeitlich modulierte Strömungen, einerseits durch eine Rohrströmung und andererseits in der Nähe einer rotierenden Scheibe. Die Genauigkeit der Ergebnisse des letzteren Falls bestätigt uns die Gültigkeit der Theorie in Bereich der Zwischenfrequenz. Im Hochfrequenz-bereich kann man eine Abweichung im Verhältnis zur Theorie feststellen. Diese Abweichung ist darauf zurückzuführen, daß der Electronentransfernicht unendlich schnell ist.

ЧАСТОТНАЯ ХАРАКТЕРИСТИКА СКОРОСТИ МАССОПЕРЕНОСА ПРИ МОДУЛИРОВАННОМ ТЕЧЕНИИ ВБЛИЗИ ЭЛЕКТРОХИМИЧЕСКИХ ДАТЧИКОВ

Аннотация—Дано численное определение переходной функции между потоком массы на микроэлектроде и градиентом скорости на стенке. Проведено прямое экспериментальное измерение этой функции как для модулированного течения в трубе, так и для модулированного течения, индуцированного вращающимся диском. Точные данные, полученные для диска, хорошо подтверждают результаты теоретических расчетов в области средних частот и свидетельствуют о наличии явного отклонения в высокочастотном диапазоне из-за конечной скорости переноса электронов.